Regular and chaotic motion in axially deformed nuclei

W. D. Heiss,[1] R. G. Nazmitdinov,[1,2] and S. Radu[1]
[1]*Centre for Nonlinear Studies and Department of Physics, University of the Witwatersrand, PO Wits 2050, Johannesburg, South Africa*
[2]*Bogoliubov Laboratory of Theoretical Physics, Joint Institute for Nuclear Research, 141980 Dubna, Russia*
(Received 21 July 1995)

The combined effect of an octupole and hexadecapole term, when added to a strongly deformed axial harmonic oscillator potential, is carefully studied. The problem is nonintegrable, which calls for a thorough classical analysis in order to understand the quantum mechanical results. Shell structure which is found for particular combinations of the deformation parameters are explained in terms of dominant classical periodic orbits. Using the "removal of resonances" method as an approximation, explicit expressions in terms of the deformation parameters are obtained for effective winding numbers, which in turn generate the quantum shell structure. A mutual cancellation of the octupole and hexadecapole deformation in prolate superdeformed systems has been discovered. Strongly oblate deformed potentials can yield shell structure only when even higher multipoles are added while prolate potentials can support shell structure for arbitrary higher multipoles.

PACS number(s): 21.60.Cs, 05.45.+b, 24.60.Lz

I. INTRODUCTION

During the last decade the problem of order and chaos has attracted growing interest within the physics community. The subject of a quantum mechanical analogue of a classically chaotic system is one of the topical questions of physics. If the classical system is integrable, it is usually due to symmetries of the Hamilton function giving rise to first integrals. These, in turn, give rise to quantum numbers. Classical systems that are nonintegrable show generically chaotic behavior. Manifestation of a chaos in deterministic systems is reflected in properties of the corresponding quantum system in that lesser or no quantum numbers exist.

Many phenomena observed in a many body system like nuclei and metallic clusters can be explained by the mean field approach. The quantization of a system of fermions moving in a common potential leads to a bunching of levels in the single-particle spectrum, known as shells. In an integrable case the higher symmetry can cause a high degree of degeneracy of the quantum eigenstates. Consequently, a spherical symmetry leads to very strong shell effects manifested in the stability of the noble gases, nuclei, and metallic clusters (see for review [1–3]). The high level density around the Fermi level corresponds to a less stable system. When a spherical shell is only partially filled, a breaking of spherical symmetry, resulting in an energy gain, can give rise to a deformed equilibrium shape. Notice that the basic concept of the deformation in the mean field approach is the Jahn-Teller effect [4], the mechanism proposed for the first time for molecules, which leads to a spontaneous symmetry violation (see discussion in [5]). Super- and hyperdeformed nuclei are among the most fascinating examples where deviations from the spherical shape are a consequence of strong shell closures giving rise to largest level bunching (largest degeneracy or lowest level density). At the same time, phenomenological potentials like Woods-Saxon and the modified Nilsson model without a spin-orbit term are successfully used for an analysis of the properties of metallic clusters [6–8]. Naturally, the shell numbers have to be larger than the ones used in nuclear physics in accordance with the larger number of valence electrons considered for metallic clusters. For mesoscopic objects like clusters, deformations are as important as in the nuclear physics context. The larger shell number can be viewed as a mean to approach the classical border line of the shell model, a view which underlines the importance of supplementing the study of quantum mechanics by classical consideration.

The need for multipole deformations higher than the quadrupole has been recognized in nuclei and in metallic clusters in numerous calculations to explain experimental data. For instance, the octupole deformed shapes still constitute an intriguing problem of nuclear structure, experimental as well as theoretical (see for review [9,10]). The hexadecapole deformation is essential for the understanding of equilibrium shapes and the fission process of super- and hyperdeformed nuclei [9,11]. In the case of metallic clusters, the axial hexadecapole deformation is important for the interpretation of experimental data in simple metals [12]. Inclusion of higher multipoles leads, however, to a nonitegrable problem. In fact, the single-particle motion turns out to be chaotic. It is expected that an increasing strength of the corresponding multipole deformation increases the amount of chaos in the classical potential as quantified by an increasing Lyapunov exponent. Accordingly, in the transition from ordered to chaotic motion the quantum numbers lose their significance, and the system behaves like a viscous fluid [13]. Therefore, a disappearance of shell structure should be expected in the analogous quantum case. However, recently the occurrence of shell structure has been reported for many body systems like nuclei and metallic clusters [14,15] at strong octupole deformation. A major conclusion of [15] is that, albeit nonintegrable, an octupole admixture to quadrupole oscillator potentials leads, for some values of the octupole strength, to a shell structure similar to a plain but more deformed quadrupole potential. This result shows that there is a tendency of the system to restore the original symmetry which is destroyed by the octupole term. In other words, we encounter the restoration of the original symmetry of the unperturbed integrable Hamiltonian under certain conditions,

although the system is nonintegrable owing to the perturbation.

The equilibrium deformation is ultimately related to the behavior of the single-particle level density of the quantum Hamiltonian. According to the semiclassical theory [16] the frequencies in the level density oscillations of single-particle spectra are determined by the corresponding periods of classical closed orbits. The short periodic orbits determine the gross shell structure, whereas contribution of longer orbits give finer details. Analysis of shell structure phenomena in nuclei in terms of classical orbits was started by the work of Balian and Bloch [17] who studied the density of eigenmodes in a spherical cavity with reflecting walls. The importance of deformed shapes for nuclei led to the generalization of this analysis in considering a deformed ellipsoidal well and a deformed harmonic oscillator [1,18,19]. Since these problems are integrable, attention was given to regular motion. One of the first attempts to analyze shell structure phenomena and chaotic motion in a quadrupole deformed diffuse cavity was given in [20].

In this paper we present results of an analysis of a more realistic but still simple model which includes the effect of higher odd and even multipoles. We hope to shed more light on this old question from a new point of view. Our approach is based on the connection between shell structure phenomena in the quantum spectrum and ordered motion in the classical analogous case. As it was mentioned above, shell structures in the quantum mechanical spectrum are related to periodic orbits of the corresponding classical problem [1,17–23]. The periodic orbits are associated with invariant tori of the Poincaré sections. If the classical problem is chaotic, the invariant tori disintegrate or disappear [24], and the shell structure of the quantum spectrum is affected by the degree of chaos [25–27].

The concept of pseudo-SU(3) symmetry [28,29] has been introduced to explain many features of superdeformed states described within a realistic nuclear potential [11,30]. In the new scheme the spin-orbit splitting appears very small and the properties of the single-particle spectrum are similar to those observed in the three-dimensional harmonic oscillator with rational ratios of the frequencies (RHO) [31–33]. Therefore, one can argue that the single-particle shell structure of RHO (which is an integrable system) should reflect the essential properties of super- and hyperdeformed nuclei. Experimentally, very little is known about multipole terms higher than hexadecapole. In this paper particular emphasis is placed upon strongly quadrupole deformed systems like superdeformed nuclei, and we concentrate only on the most important even and odd multipoles, which are quadrupole, octupole, and hexadecapole deformations. Since our interest is directed not only towards the classical but also the corresponding quantum mechanical motion, we leave out the spin-orbit term and the $(\vec{l})^2$ term present in the Nilsson model so as to render as closely as possible the analogy between the classical and quantum cases. An analysis of classical trajectories in a quadrupole deformed harmonic oscillator has shown that the spin-orbit term leads to chaotic motion [34]. Likewise, the $(\vec{l})^2$-term gives rise to chaotic behavior [22] in a quadrupole deformed potential.

Obvious differences between odd and even multipoles motivated us to study separately their respective effects upon the shell structure. Using the approach based on the "removal of resonances" method (RRM) described below we obtain good estimates for the winding numbers of classical orbits and find conditions, where the original symmetry is effectively restored. In a previous analysis of an octupole term it was demonstrated that shell structure can exist only for the prolate case [15,35], whereas for the hexadecapole term alone the shell structure occurs in prolate as well as oblate systems [26]. In this paper the complete analysis including the combined effect of odd and even multipoles will be presented.

II. RRM AND ARBITRARY AXIAL DEFORMATION

We describe an approximation method which allows, in cases to be specified, the reduction of the nonintegrable to an effective integrable problem. For the method to be successful, the system has to be sufficiently close to an integrable problem. As we shall see below, this criterium gives a guide line as to whether shell structure can or cannot be expected in the corresponding quantum mechanical cases. In cases where the method can be applied successfully, it explains the specific shell structures found quantum mechanically.

The classical approach is based on the "removal of resonances" method (RRM), which has been developed in secular perturbation theory [36] and is particularly effective for a two degrees of freedom system. The technique uses action-angle variables of the unperturbed Hamiltonian and averages over the faster phase. Usually, prior to such an operation, a canonical transformation is necessary in order to remove the initial resonance from the unperturbed Hamiltonian (in our case the axial harmonic oscillator without higher multipoles). In the new rotating frame, one of the phases will only measure the slow variation of the variables about the original resonance which now becomes a fixed elliptic point. The problem is then treated by averaging over the remaining faster phase. In the case of a super- or hyperdeformed potential though, there already appears to be a clear distinction between a slow and fast phase, therefore the canonical transformation is unnecessary. Since the Hamilton function is periodic in both angles, this approximation amounts to keeping the zero-order term of its Fourier expansion in the fast moving angle. The integration of the Hamilton function over the angles can be done analytically, which makes the approximation particularly attractive.

An axial harmonic oscillator Hamiltonian which is deformed by arbitrary multipoles has the form

$$H=\frac{1}{2m}\left(p_\rho^2+p_z^2+\frac{p_\phi^2}{\rho^2}\right)+\mathcal{U}(r,\vartheta), \tag{1}$$

where

$$\mathcal{U}(r,\vartheta)=\frac{m\omega^2}{2}\left(\rho^2+\frac{z^2}{b^2}+r^2[\lambda_3 P_3(\cos\vartheta)+\lambda_4 P_4(\cos\vartheta)+\cdots]\right) \tag{2}$$

with $r^2=\rho^2+z^2$, $\cos\vartheta=z/r$. The z component of the angular momentum is denoted by p_ϕ and $P_k(\cos\vartheta)$ is the kth order Legendre polynomial. The parameter b characterizes an ob-

late and a prolate shape for $0<b<1$ and $b>1$, respectively. For a nonvanishing $\lambda_3,\lambda_4,\ldots$ the problem becomes a nonintegrable two degrees of freedom system. Note that the only constant of motion is the total energy. The potential appearing in (2) has extensively been used in modeling nuclear [37] and metallic cluster deformations [2,38].

After rewriting the coordinates and momenta in angle-action variables the averaging is carried out directly on each individual term associated with the Legendre polynomials. The result of the averaging depends on the eveness or oddness of the polynomials and on the variable over which the averaging is carried out, which is ϑ_ρ in the prolate case and ϑ_z in the oblate case. The unperturbed action-angle variables are related to the coordinates (ρ,z) by

$$\rho=\sqrt{\frac{2J_\rho}{m\omega}}\sin\vartheta_\rho,$$

$$z=\sqrt{\frac{2bJ_z}{m\omega}}\sin\vartheta_z,$$

$$p_\rho=\sqrt{2m\omega J_\rho}\cos\vartheta_\rho,$$

$$p_z=\sqrt{\frac{2m\omega J_z}{b}}\cos\vartheta_z.$$

We use the polynomial expansion which reads for even multipoles

$$r^2P_{2k}(\cos\vartheta)=r^2\sum_{i=0}^{k}c_{2k,i}\cos^{2i}\vartheta=\sum_{i=0}^{k}c_{2k,i}\frac{z^{2i}}{(\rho^2+z^2)^{i-1}}. \tag{3}$$

In the oblate case, when the averaging is performed over ϑ_z, we obtain from the multipole r^2P_{2k}

$$\langle r^2P_{2k}\rangle_{\vartheta_z}=\frac{\xi_z^2}{\sqrt{\pi}}\sum_{i=0}^{k}c_{2k,i}\frac{(i-1/2)\Gamma(i-1/2)}{\Gamma(i+1)}\left(\frac{\xi_z^2}{\rho^2}\right)^{i-1}\times{}_2F_1\left(i-1,i+\tfrac{1}{2},i+1,-\frac{\xi_z^2}{\rho^2}\right) \tag{4}$$

with ${}_2F_1$ being the hypergeometric function. We introduced $\xi_z^2=2bJ_z/(m\omega)=2bE_z/(m\omega^2)$ where E_z and $E_\rho=E-E_z$ are the portions of the total energy E that reside in the z and the ρ motion, respectively; note that within the approximation E_z and hence E_ρ are time independent. In the prolate case, when the averaging is performed over ϑ_ρ, we obtain

$$\langle r^2P_{2k}\rangle_{\vartheta_\rho}=z^2\sum_{i=0}^{k}c_{2k,i}\,{}_2F_1\left(\tfrac{1}{2},i-1,1,-\frac{\xi_\rho^2}{z^2}\right), \tag{5}$$

where $\xi_\rho^2=2J_\rho/(m\omega)=2E_\rho/(m\omega^2)$. We mention that this time E_ρ refers to the unperturbed motion in the ρ coordinate while E_ρ as used after Eq. (4) refers to the perturbed motion; *mutatis mutandis* the same holds for E_z.

The odd multipole contribution is zero in the oblate case after averaging. In the prolate case it becomes:

$$\langle r^2P_{2k+1}\rangle_{\vartheta_\rho}=\mathrm{sgn}(z)z^2\sum_{i=0}^{k}c_{2k+1,i}\,{}_2F_1\left(\tfrac{1}{2},i-\tfrac{1}{2},1,-\frac{\xi_\rho^2}{z^2}\right). \tag{6}$$

A nonzero contribution is obtained in the oblate case when averaging is carried out over the function $r^2P_{2k+1}(\cos\vartheta)\cos\vartheta$ which corresponds to the next order term. But this does not result in a decoupling of the variables z and ρ. It follows that in the oblate case only even multipoles can decouple the potential of (2). We can therefore expect a certain degree of order, may be shell structure, when even multipoles are added to oblate quadrupole deformation. In contrast, adding significant odd multipole deformation in the oblate case is expected to produce chaotic behavior. In the prolate case, however, since the potential decouples in either situation (even and odd multipoles), we expect little or no chaotic behavior; possible shell structures can occur at particular combinations of the deformation strengths $b,\lambda_3,\lambda_4,\ldots$.

If shell structure occurs in the low-lying quantum spectrum, it must be due to the existence of a dominating short periodic classical orbit. If there is a periodic orbit whose stability island dominates the phase space, its winding number can be estimated by fixing ξ_ρ or ξ_z equal to zero, respectively. This particular choice enables analytic expressions for the winding numbers. The winding number of a periodic orbit is defined as the ratio of the frequencies of the two degrees of freedom ω_ρ/ω_z and determines the type of shell structure that occurs quantum mechanically. For instance, for $\omega_\rho/\omega_z=2$ one has the prolate superdeformed case, for $\omega_\rho/\omega_z=3$ we have the prolate hyperdeformed case, etc.

Within the approximation ω_z and ω_ρ are unchanged in the oblate and prolate case, respectively. In the oblate case, the motion in ρ is described for $\xi_z=0$ by the effective potential

$$W_{\mathrm{eff}}(\rho)=\frac{m\omega^2\rho^2}{2}\left(1+\sum_{k\geq 2}\lambda_{2k}c_{2k,0}\right)+\frac{p_\phi^2}{2m\rho^2}. \tag{7}$$

From the frequency of the motion in this potential we obtain the winding number

$$\frac{\omega_\rho}{\omega_z}=b\sqrt{1+\sum_{k\geq 2}\lambda_{2k}c_{2k,0}}. \tag{8}$$

In the prolate case, at $\xi_\rho=0$, the effective potential becomes

$$W_{\mathrm{eff}}(z)=\frac{m\omega^2z^2}{2}[\alpha+\beta\,\mathrm{sgn}(z)] \tag{9}$$

with α and β given by

$$\alpha=\frac{1}{b^2}+\sum_{k\geq 2}\sum_{i=0}^{k}\lambda_{2k}c_{2k,i}, \tag{10}$$

$$\beta=\sum_{k\geq 1}\sum_{i=0}^{k}\lambda_{2k+1}c_{2k+1,i}. \tag{11}$$

The period of the motion in the potential (9) is obtained from

$$T_z=\sqrt{2m}\int_{z_{\min}}^{z_{\max}}\frac{dz}{\sqrt{E_z-W_{\text{eff}}(z)}}, \tag{12}$$

where $z_{\min}$ and $z_{\max}$ are the boundaries of the motion and E_z is the energy in the z coordinate. It follows for the winding number

$$\frac{\omega_\rho}{\omega_z}=\frac{1}{2}\left(\frac{1}{\sqrt{\alpha^2-\beta^2}}+\frac{1}{\sqrt{\alpha^2+\beta^2}}\right). \tag{13}$$

III. CRITICAL VALUES OF THE MULTIPOLE STRENGTH PARAMETERS

Our interest is focused on the contribution of the octupole and hexadecapole deformation in super- and hyperdeformed system. Therefore, the general potential Eq. (2) is reduced to the form

$$V(\rho,z)=\frac{m}{2}\omega^2\left(\rho^2+\frac{z^2}{b^2}+\lambda_3\frac{2z^3-3z\rho^2}{\sqrt{\rho^2+z^2}}+\lambda_4\frac{8z^4-24z^2\rho^2+3\rho^4}{z^2+\rho^2}\right). \tag{14}$$

The terms multiplied by λ_3 and λ_4 give rise to octupole and hexadecapole deformations, the respective terms are proportional to $r^2P_3(\cos\vartheta)$ and $r^2P_4(\cos\vartheta)$. In this section we determine the domain of the two coupling parameters λ_3 and λ_4 for which the potential gives rise to a proper bound state problem. This is important for two reasons: (i) the corresponding quantum mechanical problem is meaningful only if tunnelling into scattering states can be excluded, and (ii) the classical problem is expected [15] to give rise to hard chaos, if the parameters approach their respective critical values for which the potential no longer binds.

The potential of Eq. (14) forms a deformed mould which tends to infinity for large values of ρ and z provided the two strength parameters λ_3 and λ_4 are sufficiently small. For specific critical values of the pair of parameters the potential will no longer tend to infinity in all directions of the ρ-z plane but towards zero in a particular direction. When either of the absolute values of the pair is increased further, the potential will tend towards minus infinity in that direction. The critical value of one parameter depends on the value of the other. In this way we obtain a critical curve in the λ_3-λ_4 plane.

We seek the particular slope α along the line $\rho=\alpha z$ where the potential $V(\rho,z)$ displays just the behavior described in the previous paragraph. Since the potential is homogeneous in its coordinates, it is sufficient to determine α so that

$$V(\alpha,1)=0. \tag{15}$$

To ensure that the potential still tends to infinity at neighboring values of the solution of Eq. (15), which means criticality, we have to require in addition the condition

$$\frac{d}{d\alpha}V(\alpha,1)=0. \tag{16}$$

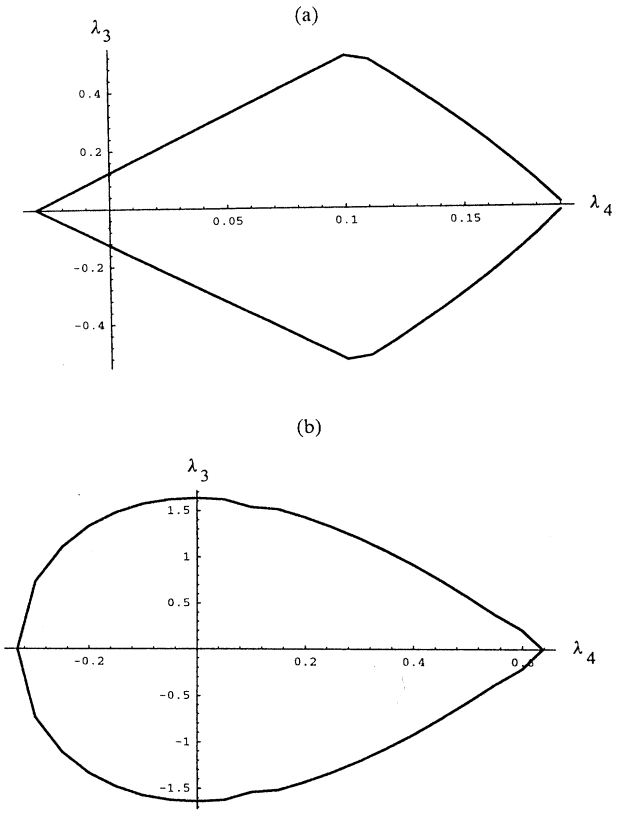

FIG. 1. Boundaries for the allowed values of the deformation parameters λ_3 (octupole strength) and λ_4 (hexadecapole strength) for which the potential binds: (a) prolate superdeformed case ($b=2$), (b) oblate superdeformed case ($b=1/2$).

Our interest is focused on the pair λ_3 and λ_4 which ensures the simultaneous fulfilment of Eqs. (15) and (16). Both equations are, after some algebraic manipulations, polynomials in α. As a consequence, α can be eliminated which leads to the resultant of the two equations. The resultant is a polynomial in λ_3 and λ_4, and setting it equal to zero yields precisely the relation between the pair of the strength parameters which we are seeking: for values smaller than the absolute values obeying the relation, the potential binds, while for larger values the potential tends to minus infinity along one (or more) directions.

The general form of the resultant is rather cumbersome, the authors have calculated it using the software from *Mathematica*. The critical curves for the prolate and oblate case, which are displayed in Fig. 1, have been found numerically using these polynomials which are of sixth order in λ_3. The closed curves delineate the area within which the potential yields bound states. In the following section we seek the range where the single-particle motion yields simple periodic orbits which give rise to quantum mechanical shell structure.

IV. CLASSICAL TREATMENT

The axial symmetry of the potential given in Eq. (14) guarantees conservation of the z component of the angular momentum denoted by p_ϕ, the discussion will be focused on

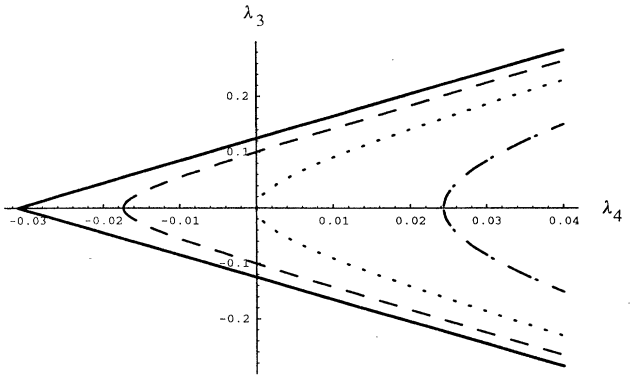

FIG. 2. Equideformation curves within the boundaries of the deformation strengths for $b=2$ and winding numbers equal to 3 (dashed line), 2 (dotted line), and 3/2 (dot-dashed line).

$p_\phi=0$ unless indicated otherwise.

In previous work results were obtained in a thorough analysis for $\lambda_4=0$ and $\lambda_3\neq 0$ [15,35] and for $\lambda_3=0$ and $\lambda_4\neq 0$ [26]. The combination of the two terms switched on simultaneously yields new insights and results which are presently reported. To facilitate the ensuing discussion we briefly recapitulate the findings of the quoted papers. When the unperturbed problem is a prolate superdeformed potential, a manifestation of chaos is barely discernible if an octupole term is added. Only when λ_3 reaches 90% of its critical value assumes the Lyapunov exponent values appreciably different from zero. In contrast, when the unperturbed problem is an oblate superdeformed potential, the onset of chaos begins already at values of $\lambda_3 \gtrsim 0.2\lambda_{\rm crit}$ and, importantly for the quanum mechanical problem, short periodic orbits occupy an insignificant portion of phase space. However, in the prolate situation, the stability islands associated with particular periodic orbits occupy a substantial portion of phase space. For special values of λ_3 such orbits turn out to have winding numbers with small numerators and denominators, and it is these short orbits that give rise to new shell structures in the corresponding quantum spectra. For instance, the values $b=2$ and $\lambda_3=0.66\lambda_{\rm crit}$ produce a spectrum which has the shell structure that resembles in all aspects the situation relating to the values $b=5/2$ and $\lambda_3=0$. The explanation for the new shell structure is found in the corresponding classical problem where for $b=2$ and $\lambda_3=0.66\lambda_{\rm crit}$ the stability island of the periodic orbit with the winding number 5/2 occupies nearly 70% of phase space. The same considerations apply even for irrational values of the quadrupole deformation b, when the unperturbed problem does not give rise to closed orbits. For instance, $b=\sqrt{3}$ and $\lambda_3=0.56$ produces essentially the situation of a plain superdeformation ($b_{\rm eff}=2$) [14,35].

While the findings of the classical problem are backed up by numerical calculations, they are primarily based on the analytical method described in the section two. For super- or hyperdeformed unperturbed potentials ($b\geq 2$) the frequency of the oscillation in the ρ coordinate is twice as fast or faster than that in the z coordinate. This feature will prevail for sufficiently small values of λ_3 and λ_4. The unperturbed Hamilton function, when rewritten in action and angle coordinates, is independent of the angles. The full Hamilton function, being a nonintegrable problem, is approximated by an effective Hamilton function that is obtained by averaging over the fast oscillating angle ϑ_ρ for the case considered.

After averaging and rewriting the action variables and the remaining angle ϑ_z in terms of the original momentum and coordinate values we obtain

$$H_{\rm av}=\frac{p_\rho^2+p_z^2}{2m}+\frac{m\omega^2}{2}\rho^2+U_{\rm eff}(z), \tag{17}$$

where

$$U_{\rm eff}(z)=\frac{m\omega^2}{2}\left\{\frac{z^2}{b^2}+\lambda_3\xi_\rho^2\frac{\mathrm{sgn}(z)}{2\pi}\left[8\frac{z^2}{\xi_\rho^2}K\left(-\frac{\xi_\rho^2}{z^2}\right)-3\pi{}_2F_1\left(\frac{1}{2},\frac{3}{2},2;-\frac{\xi_\rho^2}{z^2}\right)\right]+\lambda_4\left(\frac{3}{2}\xi_\rho^2-27z^2+\frac{35|z^3|}{\sqrt{\xi_\rho^2+z^2}}\right)\right\} \tag{18}$$

and $\xi_\rho^2=2J_\rho/(m\omega)=2E_\rho/(m\omega^2)$ which is a constant within the approximation. Here K is the first elliptic integral. Note that the approximated Hamilton function is separable in the two coordinates with the ρ motion being unperturbed. Consequently the frequencies are $\omega_\rho=\omega$ and $\omega_z=2\pi/T_z$ with

$$T_z=\sqrt{2m}\int_{z_{\rm min}}^{z_{\rm max}}\frac{dz}{\sqrt{E-E_\rho-U_{\rm eff}(z)}}. \tag{19}$$

The motion in the z coordinate is different from the unperturbed motion and its frequency depends on ξ_ρ, i.e., on the amount of the energy residing in the ρ motion. As we shall see in the following section the ξ_ρ dependence turns out to be weak and becomes significant only for ξ_ρ being near to its maximum value, which is for very small amplitudes in the z motion. Using Eq. (13) we obtain for the winding number

$$\frac{\omega_\rho}{\omega_z}=\frac{1}{2}\left(\frac{1}{\sqrt{1/b^2-2\lambda_3+8\lambda_4}}+\frac{1}{\sqrt{1/b^2+2\lambda_3+8\lambda_4}}\right). \tag{20}$$

This result is exact for $H_{\rm av}$ when $\xi_\rho=0$ (all energy resides in the z motion), but by the previous argument it applies for large part of phase space. Moreover, it serves as a useful and reliable guideline for the full problem as we shall see in the subsequent section.

While the averaging procedure does not tell us about the onset of chaotic motion, i.e., the parameter range for which the approximation is valid, we expect it to be good for small values of $|\lambda_3|$ and $|\lambda_4|$. In Fig. 2 we have inserted into the allowed area of parameter values (Fig. 1) a few curves of given constant winding numbers using Eq. (20) with $b=2$. Periodic orbits with the given winding number are expected for strength parameters which lie on the curves. It is along these curves where the corresponding quantum mechanical problem of the octupole + hexadecapole potential yields shell structures resembling the plain quadrupole deformation of the given deformation parameter, i.e., winding number. For instance, the values $b=2$, $\lambda_3=0.14$, $\lambda_4=0.02$ yield

shell structures just like $b=2$, $\lambda_3=\lambda_4=0$; also, with $b=2$ it needs $\lambda_3=0.1$ and $\lambda_4=0$ to get the same shell structures as a plain quadrupole with $b=3$ [15]. Figure 2 is drawn for $b=2$ which implies that the curve with winding number 2 must go through the origin. For this curve we have a genuine cancellation of the effect of the octupole deformation with that of the hexadecapole deformation; the former tends to increase the effective prolate deformation whereas the latter has the opposite effect. Note that the winding numbers to the left and right of the cancellation curve are larger and smaller than 2, respectively. Similar drawings are possible for different values of b in which case the statements made above apply accordingly.

In view of the subsequent discussion about shell structure it is important to note that, within the approximation, the result condensed in Eq. (20) is independent of the value of p_ϕ. In fact, a finite value of the z component of the angular momentum adds the effective term $p_\phi^2/(2m\rho^2)$ to the potential in Eq. (14) but leaves the frequency ω_ρ and ω_z unchanged. For the quantum spectrum this means an accumulation of levels of different (quantised) values of l_z (magnetic quantum number) at the same energy, which brings about the shell structure.

The oblate case ($b<1$) does not lend itself to the same approximation procedure. As was reported in [15] an octupole addition to an oblate quadrupole potential gives no contribution to the zeroth order when averaging over ϑ_z. As pointed out in Sec. II the next order can be calculated, however, no gain is made, since the two coordinates do not separate. Yet, if only a hexadecapole term is added, the same procedure can be applied and we obtain [26]

$$W_{\text{eff}}(\rho)=\frac{m}{2}\omega^2\left[\rho^2+\lambda_4\left(\frac{35|\rho^3|}{\sqrt{\rho^2+\xi_z^2}}-32\rho^2+4\xi_z^2\right)\right] \tag{21}$$

with $\xi_z^2=2bE_z/(m\omega^2)$. In this case, we find for $\xi_z=0$, using Eq. (8), for the winding number [26]

$$\frac{\omega_\rho}{\omega_z}=b\sqrt{1+3\lambda_4}. \tag{22}$$

Note that the admixture of the hexadecapole term to the oblate potential yields, quantum mechanically, an effective plain oblate case but with less deformation; for instance, $b=2/5$ and $\lambda_4=0.188$ resembles to $b=1/2$ and $\lambda_4=0$. This is in contrast to adding an octupole to a prolate potential where the effective deformation is increased. The combined effect of octupole and hexadecapole is contained in Fig. 2 for the prolate case. A corresponding drawing for the oblate case is meaningless, since the octupole admixture produces chaos for comparatively small values of λ_3.

Our findings can be generalized. As it has been shown in Sec. II, the addition of an arbitrary multipole to a prolate deformed potential is amenable to this approximative treatment. In contrast, only even multipoles lend themselves to the same treatment when added to an oblate deformed potential.

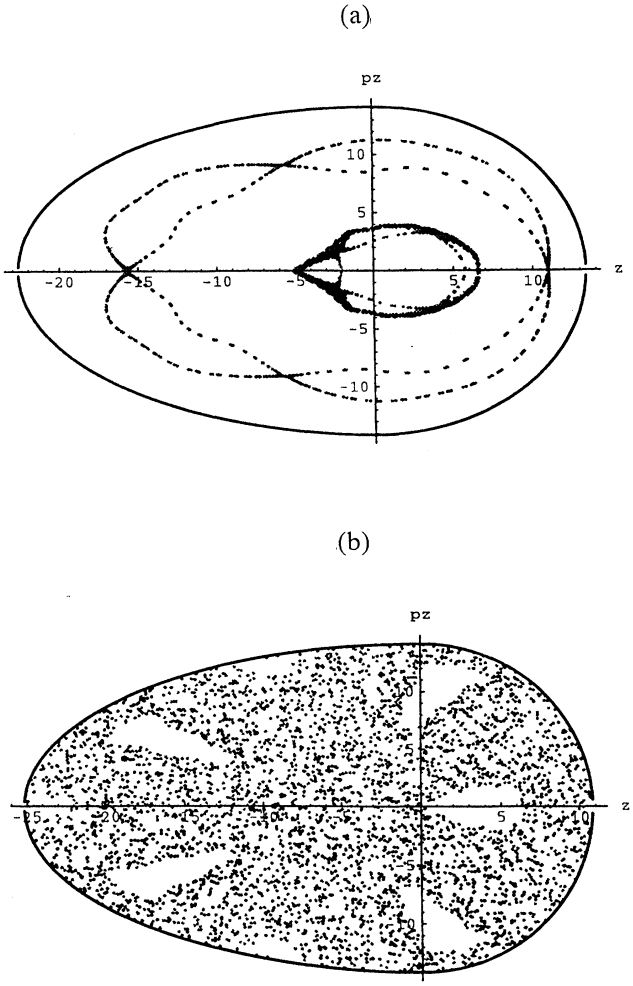

FIG. 3. Surfaces of section at special points on the superdeformation curve at $\lambda_4=0.007$ with two orbits (a) and $\lambda_4=0.02$ with one orbit (b). Both orbits in (a) contain periodic orbits with winding number 2:1 within their separatrices.

V. NUMERICAL RESULTS

A. Classical

The perturbative treatment of the previous section is expected to be reliable for sufficiently small values of λ_3 and λ_4. The actual range of its validity can only be assessed by comparison with results obtained by numerically integrating the equations of motion. Note, however, that the latter method cannot yield the insight gained from the perturbative procedure. For $b=2$ and $\lambda_4>0$ the exact and perturbative approach agree very well up to $\lambda_4\approx 0.025$. We concentrate on superdeformation ($b=2$), as this appears of special interest to experimental work.

In Fig. 3 we present surfaces of section along the cancellation curve $\omega_\rho/\omega_z=2$ for a few values of the pair (λ_3,λ_4). Since the potential scales as $V(\beta\rho,\beta z)=\beta^2 V(\rho,z)$, only one energy value has to be considered [39]. For small values the basic structure is a fourfold separatrix that hosts in its centers a periodic orbit of winding number 2. Unstable periodic orbits of the same winding number are associated with the boundary of the separatrix

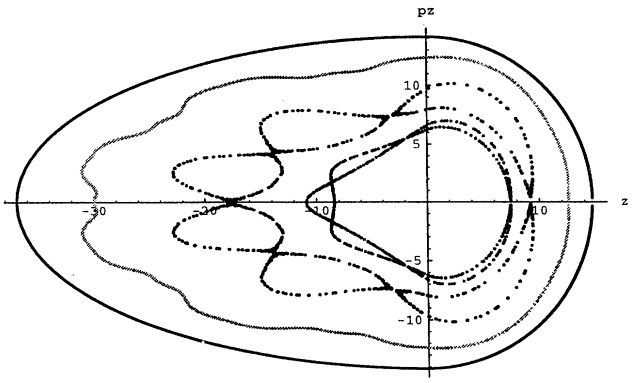

FIG. 4. Surfaces of section at $\lambda_4=-0.004$ on the hyperdeformation curve. The outer and inner separatrix correspond to the winding numbers 3:1 and 5:2, respectively. Three orbits are shown.

shown in Fig. 3(a). The corresponding Lyapunov exponent is virtually zero for this case. With increasing values of λ_4 its value increases, and so does visually the onset of chaos as illustrated in Fig. 3(b). At $\lambda_4=0.02$ [Fig. 3(b)] the Lyapunov exponent is about 0.07. All structure has disappeared in the surface of section at $\lambda_4=0.025$, where all of phase space is filled with dots. Nevertheless, a Fourier analysis of the trajectories $\rho(t)$ and $z(t)$ indicates that the dominant components still match the ratio $\omega_\rho/\omega_z\approx 2$. Only when the values of the pair (λ_3,λ_4) are further increased, is the contamination by other components too strong and the concept of winding numbers becomes meaningless. Also the Lyapunov exponent is larger than 0.1 for $\lambda_4>0.025$. Here we enter the region, where the perturbative approach fails. As we discuss below, shell structure occurs in the quantum spectrum up to this point.

For negative λ_4 the winding number is larger. Orbits with $\omega_\rho/\omega_z=3$, which is hyperdeformation, are expected from perturbation and they are indeed found. However, the motion depends on the initial conditions, i.e., on ξ_ρ, to a much greater extent than in the cases discussed above. For instance, for $\lambda_4=-0.004$ we obtain orbits with appreciable stability islands in agreement with hyperdeformation, but, as is illustrated in Fig. 4, in addition to the orbit with winding number 3 there is a further orbit with winding number 5/2 whose stability islands occupy a significant portion towards the center of phase space. Further outside orbits with winding numbers between 3 and 7/2 dominate. Recall that the curves in Fig. 2 are drawn for $\xi_\rho=0$, and only when there is a weak dependence on ξ_ρ can we expect a plain shell structure in the quantum spectrum. As we see below it turns out in the quantum mechanical results that hyperdeformed shell structure is not as clearly seen for $\lambda_4<0$, since there is interference with additional periodic orbits.

From Sec. II we know that, in the oblate case, the perturbative treatment does not apply for deformations with odd multipoles. In [26] dominant periodic orbits and shell structure associated with it have been shown to exist in strongly deformed cases ($b=2/5$) for certain values of λ_4 and $\lambda_3=0$. The admixture of an octupole to the hexadecapole term produces chaos in oblate situations to the extent that no shell structure can emerge in the quantum case.

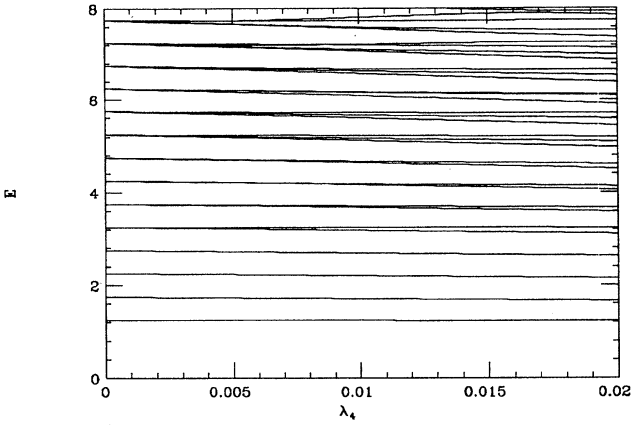

FIG. 5. Energy levels calculated along the cancellation curve for $b=2$.

B. Quantum mechanical

The quantum mechanical results are in line with the classical predictions. We calculated the energy levels of the Hamiltonian

$$H=H_0+\lambda_3 H_3+\lambda_4 H_4, \tag{23}$$

where the diagonal matrix H_0 comprises the axial harmonic oscillator, and H_3 and H_4 are the octupole and hexadecapole terms, respectively. The consistent calculation of the matrix elements in a truncated basis is described in [15].

From the discussion in the previous subsection one should expect that the quantum mechanical spectrum, as far as the shell structure is concerned, does not depend on the variation of the pair (λ_3,λ_4) when moving along the cancellation line. This is nicely confirmed for the lower end of the spectrum in Fig. 5 where the levels are plotted versus λ_4 along the curve $\omega_\rho/\omega_z=2$ for $b=2$. The levels refer to zero magnetic quantum number. Note that the levels up to around $\lambda_4=0.016$ form basically the same pattern as the ones at $\lambda_4=0$. This is a clear indication that for $0\leq\lambda_4\leq 0.016$ the effective deformation remains virtually constant and equal to 2. For $\lambda_4>0.016$ the shell structure disintegrates. The value $\lambda_4=0.016$ on the cancellation curve corresponds to $\lambda_3=0.12$ which would yield an effective deformation larger than 3 without the hexadecapole contribution; this clearly underlines the cancellation effect. Note also that in Fig. 5 the lifting of the degeneracies appears to be quadratic in λ_4, since λ_4 is varied along the cancellation curve. At the origin λ_3 depends on λ_4 as $\sim\sqrt{\lambda_4}$ which gives rise to the effective quadratic dependence. According to the authors of [40] such behavior signals suppression of chaos as is discussed in the following section.

We illustrate in Fig. 6 the square of the modulus of the Fourier transform of the quantum level density, i.e., the expression $|\Sigma\exp(iE_nt)|^2$, for $\lambda_4=0.01$ and $\lambda_3=0.09$ which is a point on the cancellation curve with $b=2$. We consider $l_z=0$, larger values of l_z are addressed below. The distinct peaks near to $T=8$, 16, 24, 32, and 40 correspond to the major classical periodic orbit which determines the shell structure along the cancellation curve. For lesser values of

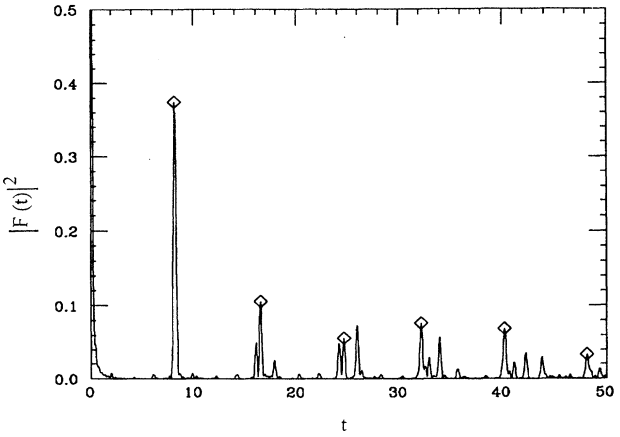

FIG. 6. Modulus squared of the Fourier transform of the level density for $b=2$ on the cancellation curve at $\lambda_4=0.01$. The recurring peaks corresponding to the dominant periodic orbit are marked by a diamond.

λ_4 the peaks would be more pronounced while for larger values other contributions would make the recurrent peaks less and less discernible. Note that the heights of the recurrent peaks under discussion do not uniformly decrease, in fact their envelope is the Fourier transform of the spreading distribution [41] of the levels which emerge from the degenerate levels under the influence of the octupole and hecadecapole contributions. This explains why the envelope of the peaks changes with λ_4 while their positions remain unchanged. In line with the approximation the peaks should be independent of l_z, in reality there is a slight l_z dependence. Yet, it is sufficiently weak to allow the formation of proper shell structure which implies a bunching of levels of different magnetic quantum numbers. This is addressed in the following.

As a quantitative measure for shell structure we use the Strutinsky-type analysis [42] introduced in [15]. The total energy $E_{\rm tot}(\lambda,N)$ which is the sum over all single-particle levels up to N is fitted by a polynomial $E_{\rm smooth}(\lambda,N)=\Sigma_{i=0}^{4}c_i(\lambda)N^{i/3}$, and the fluctuation $\delta E(\lambda,N)=E_{\rm tot}(\lambda,N)-E_{\rm smooth}(\lambda,N)$ is plotted versus λ and N. In this analysis all magnetic quantum numbers which can occur for the energies considered have been taken into account. From the quantity $\Delta E(\lambda,N)=\delta E(\lambda,N+1)+\delta E(\lambda,N-1)-2\delta E(\lambda,N)$ we obtain the precise location of the magic numbers. We have chosen $\lambda_4=0.007$, 0.02, 0.03 on the cancellation curve as examples. The magic numbers coincide with the plain prolate superdeformed case as illustrated in Fig. 7 and the agreement is striking. For $\lambda_4>0.025$ the shell structure disappears. An example is given in Fig. 7(c) where the corresponding magic numbers are calculated for $\lambda_4=0.03$ on the cancellation curve. Now the deviation begins to set in from the higher end of the spectrum.

At negative values of λ_4 the perturbation analysis suggests the presence of hyperdeformation along the classical hyperdeformation curve. Results are displayed in Fig. 8 for $\lambda_4=-0.002$ and -0.004. In line with the discussion in the previous subsection the shell structure pertaining to the hyperdeformed case is present but somewhat contaminated. A qualitative explanation for this must be sought in the discussion referring to Fig. 4, but we cannot offer as of yet a satisfactory quantitative explanation. For larger values of the modulus of λ_4 the shell structure essentially disappears. The curves referring to winding numbers larger than 3 lie too close to the critical boundary with the consequence that the agreement between the actual orbits and perturbation results

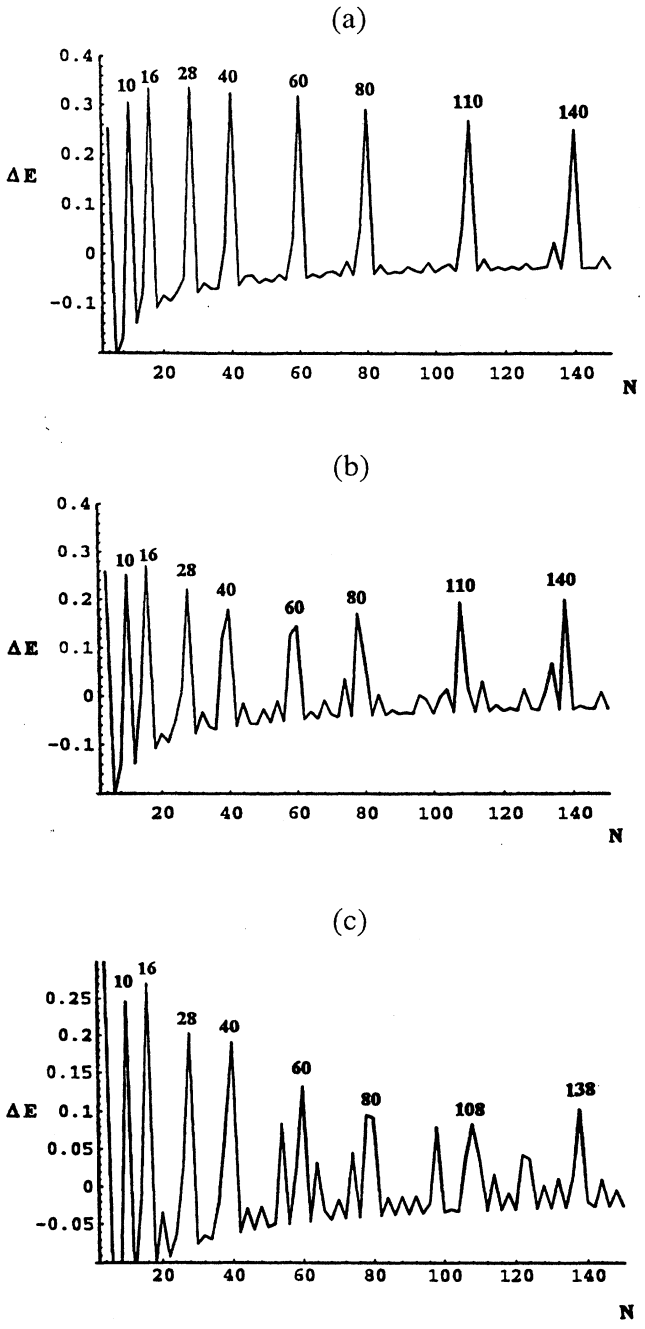

FIG. 7. Magic numbers calculated at special points on the cancellation curve for $\lambda_4=0.007$ (a), 0.02 (b), 0.03 (c). The magic numbers corresponding to a pure superdeformed case are indicated in (a) and (b), deviations occur in (c).

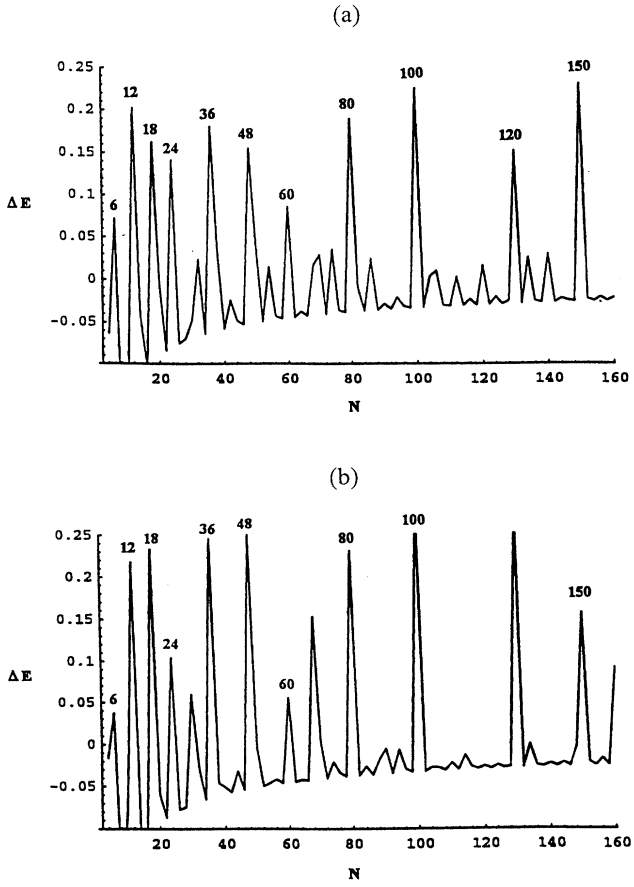

FIG. 8. Magic numbers calculated on the hyperdeformation curve at $\lambda_4=-0.002$ (a) and -0.004 (b).

is poor. For $b=2$ and $\omega_\rho/\omega_z>3$ there is virtually no shell structure.

In accordance with the discussion above, the oblate superdeformed potential produces chaos when the octupole term is switched on. The quantum spectrum has the level statistics ascribed to quantum chaos [25]. The hexadecapole term alone does give rise to new shell structure as was reported earlier [26] where, for instance, for $b=2/5$ and $\lambda_4\approx 0.1$ oblate superdeformation, i.e., $\omega_\rho/\omega_z=1/2$ was established. This is close to the value given by Eq. (22), the difference is explained in [26].

VI. EXCEPTIONAL POINTS

The discussion of the previous sections not only relates the quantum mechanical shell structure with the major periodic orbits of the classical (chaotic) system, but it also provides for an understanding of the fact that shell structure cannot occur when odd multipole terms are added to a spherical or oblate deformed harmonic oscillator. In this section we discuss, in terms of the properties of the quantum mechanical operators alone, a yet deeper explanation for this result. The analysis is based on a study of the exceptional point structure for the different cases under consideration [40].

Exceptional points are singularities [43] of the energy in the complex λ_3 or λ_4 plane. In this section we will briefly refer to the λ plane as we consider analytic continuation of the spectrum only in one of the two variables. The exceptional points are the values of λ where any two energy levels $E_n(\lambda)$ of the general problem $H_0+\lambda H_1$ coalesce when they are continued into the complex plane. They are square root branch points, and they have physical significance, since an avoided level crossing for real λ values is associated with a complex conjugate pair of exceptional points. The connection between the occurrence of avoided level crossings and exceptional points is similar in nature to the connection between the complex poles of a scattering function and the resonance structure of a cross section. In the same way as the poles of the scattering function give rise to the shape of the cross section, the exceptional points bring about the shape of the spectrum. Their interplay alone provides the mechanism for the signature of chaos in a quantum system. With the aid of exceptional points, criteria for quantum chaos can be found even when the classical counterpart does not exist [43].

The energy levels are obtained by solving the usual secular equation:

$$\det(E-H_0-\lambda H_1)=0. \tag{24}$$

To enforce coalescence of the roots of Eq. (24) the additional equation

$$\frac{d}{dE}\det(E-H_0-\lambda H_1)=0 \tag{25}$$

must be solved simultaneously. Since the Hamilton operator is irreducible with respect to symmetries, the fulfilment of the two equations simultaneously is generically excluded for real λ, as this would mean a genuine degeneracy for two levels. It has been established that a high density of exceptional points is a prerequisite for the signature of chaos in the energy spectrum [43]. It means that for the values of λ, where the density of the exceptional points and therefore that of the avoided level crossings is high, the energy spectrum generically obeys the level statistics of quantum chaos.

As a demonstration we present the results of the analysis where only the octupole term is added to the quadrupole deformed oscillator. The huge number of exceptional points, there are $N(N-1)$ exceptional points for an N-dimensional matrix problem, makes an explicit determination of their positions prohibitive. However, only their distribution is of interest and this is determined using the method described in [43,40]. In Fig. 9 we display the distributions of the real parts of the exceptional points as a function of λ_3 for $\lambda_4=0$. For the oblate case, illustrated in Fig. 9(b), the bulk of the exceptional points occurs immediately when λ_3 is switched on. This signals the immediate onset of chaos thus preventing formation of shell structure. In contrast, as is illustrated in Fig. 9(a), the bulk of the exceptional points occurs for the prolate case for much larger values of λ. For the matrix problem considered the bulk appears at $\lambda>\lambda_{\text{crit}}$, which is beyond the region of physical interest.

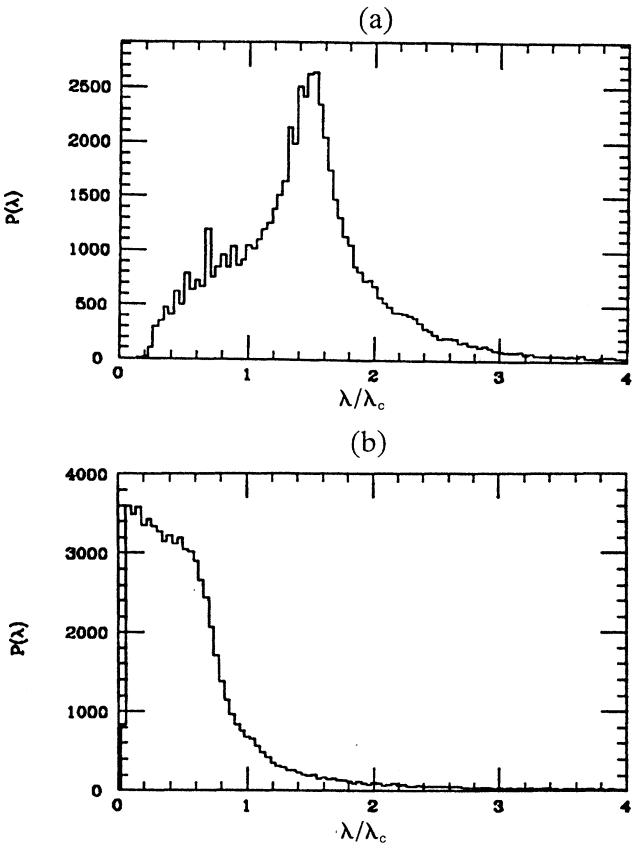

FIG. 9. Distribution of the real parts of the exceptional points versus λ/λ_{crit} for the prolate case (a) and the oblate case (b).

The explanation for this pattern lies in the different matrix structure of the two cases. The first-order perturbation term vanishes in the prolate problem. As a result, the spectrum has a zero derivative at $\lambda=0$. It is described in detail in [40] that, as a consequence, exceptional points cannot occur near to $\lambda=0$, as a matter of fact most occur beyond λ_{crit}. Here we point out that the entries of zeros in the blocks relating to the degenerate subspaces of the unperturbed problem are the basic cause for this feature. In contrast, the occurrence of avoided level crossings near to $\lambda=0$ is not prohibited for the oblate case, since now the matrix blocks referred to above are filled thus producing a large number of exceptional points around $\lambda=0$. This brings about the onset of chaos for $0<\lambda<\lambda_{crit}$. While this was explained in previous sections by the classical analysis, we see here the corresponding mechanism of the quantum mechanical matrix problem at work. It is the matrix structure alone which causes the different distributions of the exceptional points with the consequence that the prolate case exhibits considerably less chaos for small values of λ than the oblate case.

The actual formation of shell structure in the prolate case has not been explained as of yet by exceptional points. In this context we wish to stress the connection between the symmetry breaking mechanism and the very specific distribution of level repulsions: the system aspires to break the spherical symmetry where the density of avoided level crossings is high, so as to attain a new order and stability as manifested by regions of low level density.

VII. SUMMARY

In 1960 it was suggested by Gelikman [44] that strongly deformed nuclei could occur because of the formation of new shell structure. Nowadays super- and hyperdeformed nuclei are one of the challenging problems of nuclear structure. They appear to be one of the physical situations where our modern understanding of nonlinear phenomena, which implies the interplay between regular and chaotic motion, can be tested.

We have investigated the shell structure produced by a strongly deformed axial harmonic oscillator with an octupole and hexadecapole term. When either the octupole or hexadecapole term is switched on, the original symmetry of the unperturbed Hamiltonian (RHO) and the degeneracy associated with it is destroyed. Using the classical method RRM we effectively reduce the nonintegrable problem to an integrable case, which is in our case the two-dimensional oscillator with new effective frequencies. The method is succesful when the system is sufficiently close to integrability, which may happen even when, for instance, the octupole term is fairly large. We see here the KAM theorem nicely at work in that the invariant tori turn out to be rather stable and therefore can support the regular motion of the nonintegrable problem; we are faced with a typical case of soft chaos [24]. Although such situations are often the more delicate ones, we are fortunate to find good estimates via Eq. (20) for the winding numbers of the shortest classical orbits. They define the gross shell structure. As a consequence we find the conditions where the original symmetry, i.e., the RHO symmetry, is approximately restored.

There is remarkable agreement between the manifestation of shell structure for values of the strength parameters λ_3, λ_4, which coincide with the ones predicted by the RRM and give rise to stability islands on the Poincaré surfaces of sections. One of the results of this work is the occurence of shell structure in a strongly oblate deformed potential when a hexadecapole term is added. This is of interest as the adding of an octupole term produces chaos without structure. According to the RRM only even multipoles can decouple the potential of Eq. (1) for an oblate deformation. Therefore, shell structure can be supported for strongly oblate deformed nuclei only by even multipoles. This conclusion was corroborated by the analysis of exceptional points which relate to the occurrence of avoided level crossings in quantum spectra. It appears that, in the oblate case, the bulk of exceptional points, i.e., level repulsions, which provide the mechanism for the signature of chaos in a quantum system, emerge in the physically relevant region. This is in contrast to the prolate case, where they occur essentially outside the physical region.

A further interesting result is the mutual cancellation of the octupole and hexadecapole contribution in the quadrupole deformed system. The RRM allows to determine the range of parameters of λ_3 and λ_4 where the corresponding quantum mechanical problem of the quadrupole + octupole + hexadecapole potential yields shell structure resembling the plain quadrupole deformation. Along this curve the octupole deformation tends to increase the effective prolate de-

formation whereas the hexadecapole term produces the opposite effect. In fact, the hexadecapole term can stabilize the octupole deformation in superdeformed nuclei, since the cancellation curve attains values of λ_3 which are larger than its critical value for $\lambda_4=0$. We may speculate that prolate superdeformed nuclei with rather strong octupole deformation could therefore exist. In this context we stress that shell structure as manifested experimentally by specific magic numbers cannot be directly associated with a definite type of deformation of the system. For instance, within our model similar superdeformed shell patterns can be reproduced in the prolate case with a combination of less quadrupole + octupole deformations [15], or with a more deformed quadrupole system and a hexadecapole admixture [26], or with superdeformed + octupole + hexadecapole deformations. Further experimental information extracted from electromagnetic transitions is needed to distinguish between the plain superdeformed and the stronger or weaker deformed system which includes higher multipoles. Finally we comment that even though the quantum mechanical treatment shows a certain degree of suppression of classical chaos, the occurrence of a new shell structure which differs from the unperturbed case is clearly brought about by the nonlinear character of the problem. The pattern emerges when the original symmetry of the unperturbed Hamiltonian is restored even though the problem is nonintgrable due to the higher odd and even multipoles.

Our analysis is based on a rather simple model, and it is true that a realistic single-particle spectrum is poorly reproduced by the harmonic oscillator. However, the lucidity and transparence of the RHO model in describing the phenomena of extreme deformations is superior to any realistic model. From historical experience we know that simple models can be of great relevance for the understanding of real nature.

R.G.N. acknowledges financial support from the Foundation for Research Development of South Africa as well as the warm hospitality that he enjoyed during his visit to the Department of Physics of the University of the Witwatersrand.

[1] A. Bohr and B.R. Mottelson, *Nuclear Structure* (Benjamin, New York, 1975), Vol. 2.
[2] W.A. Heer, Rev. Mod. Phys. **65**, 611 (1993).
[3] M. Brack, Rev. Mod. Phys. **65**, 677 (1993).
[4] H.A. Jahn and E. Teller, Proc. R. Soc. **A161**, 220 (1937).
[5] P.-G. Reinhard and E.W. Otten, Nucl. Phys. **A420**, 173 (1984).
[6] K. Clemenger, Phys. Rev. B **32**, 1359 (1985).
[7] H. Nishioka, K. Hansen, and B.R. Mottelson, Phys. Rev. B **42**, 937 (1990).
[8] V.O. Nesterenko, Sov. J. Part. Nucl. **23**, 726 (1992).
[9] S. Åberg, H. Flocard, and W. Nazarewicz, Annu. Rev. Nucl. Part. Sci. **40**, 439 (1990).
[10] I. Ahmad and P. Butler, Annu. Rev. Nucl. Part. Sci. **43**, 71 (1993).
[11] J. Dudek, Prog. Part. Nucl. Phys. **28**, 131 (1992).
[12] Th. Hirschmann, M. Brack, and J. Meyer, Ann. Phys. **3**, 336 (1994).
[13] J. Blocki, J.-J. Shi, and W.J. Swiatecki, Nucl. Phys. **A554**, 387 (1993).
[14] K. Arita, Phys. Lett. B **312**, 123 (1994).
[15] W.D. Heiss, R.G. Nazmitdinov, and S. Radu, Phys. Rev. B **51**, 1874 (1995).
[16] M.C. Gutzwiller, J. Math. Phys. **12**, 343 (1971).
[17] R. Balian and C. Bloch, Ann. Phys. (N.Y.) **69**, 76 (1972).
[18] V.M. Strutinsky and A.G. Magner, Sov. J. Part. Nucl. **7**, 138 (1976).
[19] V.M. Strutinsky, A.G. Magner, S.R. Ofengenden, and T. Dossing, Z. Phys. A **283**, 269 (1977).
[20] R. Arvieu, F. Brut, J. Carbonell, and J. Touchard, Phys. Rev. A **35**, 2389 (1987).
[21] H. Frisk, Nucl. Phys. **A511**, 309 (1990).
[22] W.D. Heiss and R.G. Nazmitdinov, Phys. Rev. Lett. **73**, 1235 (1994).
[23] K. Arita and K. Matsuyanagi, Kyoto University Report No. KUNS 1339, 1995.
[24] M.C. Gutzwiller, *Chaos in Classical and Quantum Mechanics* (Springer, New York, 1990).
[25] W.D. Heiss, R.G. Nazmitdinov, and S. Radu, Phys. Rev. Lett. **72**, 2351 (1994).
[26] W.D. Heiss, R.G. Nazmitdinov, and S. Radu, Phys. Rev. C **52**, 1179 (1995).
[27] K. Arita and K. Matsuyanagi, Prog. Theor. Phys. **91**, 723 (1994).
[28] R.D. Ratha-Raju, J.P. Draayer, and K.T. Hecht, Nucl. Phys. **A202**, 433 (1973).
[29] J.P. Draayer, Nucl. Phys. **A520**, 259c (1990).
[30] J. Dudek, W. Nazarewicz, Z. Szymanski, and G.A. Leander, Phys. Rev. Lett. **59**, 1405 (1987).
[31] T. Bengtsson, M.E. Faber, G. Leander, P. Möller, M. Ploszajczak, I. Ragnarsson, and S. Åberg, Phys. Scr. **24**, 200 (1981).
[32] I. Ragnarsson, Phys. Rev. Lett. **62**, 2084 (1989).
[33] W. Nazarewicz and J. Dobaczewski, Phys. Rev. Lett. **68**, 154 (1992).
[34] P. Rozmej and R. Arvieu, Nucl. Phys. **A545**, 497c (1992).
[35] W.D. Heiss, R.G. Nazmitdinov, and S. Radu, Phys. Scr. **T56**, 182 (1995).
[36] A.J. Lichtenberg and M.A. Liebermann, *Regular and Stochastic Motion* (Springer, New York, 1981).
[37] S.G. Nilsson, C.F. Tsang, A. Sobiczewski, Z. Szymanski, S. Wycech, C. Gustafson, I.-L. Lamm, P. Möller, and B. Nilsson, Nucl. Phys. **A131**, 1 (1969).
[38] S.M. Reimann and S. Frauendorf, Zentralinstitut für Kernforschung Report No. FZR-58, Rosssendorf, 1994.
[39] L.D. Landau and E.M. Lifshitz, *Mechanics* (Pergamon Press, Oxford, 1976).
[40] W.D. Heiss and S. Radu, Phys. Rev. E **52**, 4762 (1995).
[41] W.D. Heiss and M. Müller, Phys. Rev. A **48**, 2558 (1993).
[42] V.M. Strutinsky, Nucl. Phys. **A122**, 1 (1968).
[43] W.D. Heiss and A.L. Sannino, J. Phys. A **23**, 1167 (1990); A.A. Kotzé and W.D. Heiss, *ibid.* **27**, 3059 (1994).
[44] B.T. Gelikman, *Proceedings of the International Conference on Nuclear Structure*, Kingston, 1960 (University of Toronto Press, Toronto, 1960), p. 874.